Supporting Information

Jha and Udgaonkar 10.1073/pnas.0905744106

SI Text

TNB-labeling and Protein Quantification. The TNB-labeled proteins were obtained by incubating the GdnHCl-unfolded protein with a 100-fold molar excess of 5, 5′-dithiobis (2-nitrobenzoic acid) (DTNB) in 6 M GdnHCl at pH 8.5. After completion of the reaction, the labeled protein was separated from free dye and GdnHCl by the use of a PD-10 column (GE Health Care Life Sciences). All of the proteins were found by mass spectrometry to be >98% labeled, with an expected 196 Da increase in the mass because of the addition of the TNB moiety.

Protein concentrations were determined by measurement of the absorbance at 280 nm, using an extinction coefficient of 14,600 M^{-1} cm^{-1} for the unlabeled proteins (1). Because the TNB group contributes to the absorbance measured at 280 nm, a correction for its contribution was done for the labeled proteins, as described earlier (2).

Reagents, Chemicals, Buffers, and Experimental Conditions. All chemicals and reagents were obtained from Sigma (unless otherwise mentioned) and were of the highest purity grade. GdnHCl (ultrapure grade) was from GE Health Care Life Sciences. The native buffer used in all of the experiments was 20 mM Tris and 250 μM EDTA at pH 8. The unfolding buffer was native buffer containing 3–8 M GdnHCl. One mM DTT was also present in all of the unlabeled protein solutions. The concentration of a GdnHCl solution was determined by measurement of the refractive index on an Abbe-type refractometer. All buffers and solutions were filtered through 0.22-μm filters before use. All of the experiments were carried out at 25 °C.

ANS-binding Experiments. Thirty μL unlabeled native protein of the desired concentration were mixed with 270 μL unfolding buffer containing the desired amount of ANS, inside the stopped-flow mixing module (SFM-4) from Biologic. The concentration of GdnHCl after the mixing was 4 M. The dead-time of mixing was approximately 6.2 ms. ANS fluorescence was excited at 350 nm, and emission was measured using a 450 nm band-pass filter. To confirm that ANS does not bind to native and unfolded proteins, 30 μL unlabeled native protein of the desired concentration were mixed with 270 μL native buffer containing the desired amount of ANS, and 30 μL unlabeled unfolded protein of desired concentration were mixed with 270 μL unfolding buffer containing the desired amount of ANS, in separate control experiments, inside the SFM-4 mixing module. The reactions were monitored as described above.

Extraction of Energy Transfer Parameters and Determination of D–A Distances. The efficiency of energy transfer, E, is determined experimentally as

$$E = 1 - \frac{F_{DA}}{F_D} \qquad [S1]$$

where F_D is the fluorescence of the donor in the absence of the acceptor (in the unlabeled protein), and F_{DA} is the fluorescence of the donor in the presence of the acceptor (in the corresponding TNB-labeled protein) (3).

The distance, R, separating the donor and the acceptor, is related to the energy transfer efficiency, E, by Förster's relation as

$$R = R_0 \left[\frac{1 - E}{E} \right]^{\frac{1}{6}} \qquad [S2]$$

The value of R_0, the Förster's distance, can be determined by using the equation:

$$R_0 = 0.211 [Q_D J \kappa^2 n^{-4}]^{\frac{1}{6}} \qquad [S3]$$

In Eq. **S3**, Q_D is the quantum yield of donor fluorescence, J is the overlap integral, κ^2 is the orientation factor, and n is refractive index of the medium (3).

The various parameters in Eq. **S3** can be determined experimentally. For the determination of the Q_D values of the N and U forms, use was made of the fact that under conditions similar to those used in this study, the fluorescence lifetime of free tryptophan is 2.6 ns, and its quantum yield is 0.14 (4). Because Q_D is proportional to fluorescence lifetime, and the fluorescence lifetime of the N state of MNEI is ≈2.45 ns, the Q_D of the N state was determined to be 0.133. Using this value for the Q_D of the N state, and the ratio of the area under the fluorescence emission spectrum of U to the area under the fluorescence emission spectrum of N (Fig. 1 *B* and *C*), the Q_D of the U state was determined to be 0.128.

The overlap integral, J, is defined as the spectral overlap between the fluorescence emission spectrum of the donor and the absorbance spectrum of the acceptor, and is given by,

$$J = \frac{\int F(\lambda)\epsilon(\lambda)\lambda^4 d\lambda}{\int F(\lambda)d\lambda} \ (M^{-1}cm^{-1}(nm)^4) \qquad [S4]$$

The fluorescence emission spectra, $F(\lambda)$, of both the unlabeled proteins and the absorption spectra, $\varepsilon(\lambda)$, of both the TNB-labeled proteins in the N and U states were measured (Fig. S1), and the value of J was determined for each FRET pair. These values are listed in Table S1.

The value of the refractive index, n, of the medium was determined to be 1.33 in 0 M GdnHCl, and 1.4 in 4 M GdnHCl. The value of the orientation factor, κ^2, depends on the relative orientation of the transition dipoles of the donor, W4, and the TNB acceptor. If the donor and acceptor are oriented randomly with respect to each other, the value of κ^2 is 2/3 (3, 5). This condition is typically met when at least one of the two chromophores is rotating freely at rates faster than the fluorescence decay rate. The rotational dynamics of the donor and both the acceptors were measured experimentally, by the measurement of the fluorescence anisotropy decay kinetics (Fig. S2). The donor as well as the acceptors seem to rotate freely (see below), and using a value of two-thirds for κ^2 appears reasonable. The observation that the intrinsic quantum yield of W4 in MNEI is 0.133 and 0.128 in the N and U states, respectively, which is similar in value to that of free tryptophan (4, 6), also suggests that W4 rotates freely and does not interact with the rest of the protein. The values of the Förster's distance, R_0, and the D–A distances, R, for both the TNB-labeled proteins, are listed in Table S1.

Time-Resolved Fluorescence-Anisotropy Measurements. In the determination of distances using FRET, there are often many concerns about the value of κ^2. Significant error might be introduced, if the orientation of transition dipoles is fixed. At present, there is no direct way to measure κ^2. It is, however, possible to set the upper and lower limits on the range of κ^2 values, which can be used to set limits on the range of possible D–A distances (3). This finding can be done by the measurements of the decays of fluorescence anisotropies of the donor and acceptor probes. The fluorescence

anisotropy decay kinetics was measured for the donor and both the acceptors (Fig. S2), as described previously (7), to obtain a range of possible values for κ^2.

For the donor W4 in the N state, 2 rotational correlation times, 0.1 ns (46% amplitude) and 4 ns (54% amplitude) were observed (Fig. S2A). In the U state (4 M GdnHcl) also, two rotational correlation times, 0.1 ns and 1 ns, were observed with corresponding amplitudes of 60% and 40%, respectively (Fig. S2A). In both cases, the value of the fundamental anisotropy, r_0, when determined by the extrapolation of the observed anisotropy decay kinetics to $t = 0$, is ≈ 0.27. For acceptor measurements, because TNB is not fluorescent, both the thiol sites were labeled by the fluorescent probe 1,5-IAEDANS [5-(amino)-naphthalene-1-sulphonic acid], as described in ref. 7. Typically, in the N state of both the IAEDANS-labeled proteins, 2 rotational correlation times, ≈ 0.2 ns ($\approx 48\%$ amplitude) and 5 ns (52% amplitude) were observed (Fig. S2 B and C). In the U state (4 M GdnHCl) also, two rotational correlation times, ≈ 0.2 ns and 1 ns, were observed with corresponding amplitudes of $\approx 60\%$ and 40%, respectively (Fig. S2 B and C). In all of the cases, the value of the fundamental anisotropy, r_0, when determined by the extrapolation of the observed anisotropy decay kinetics to $t = 0$, is ≈ 0.33. The anisotropy decay kinetics of the donor in the unlabeled proteins and the thiol sites in the IAEDANS-labeled proteins in 2 M GdnHCl are similar to what the anisotropy decay kinetics are in 4 M GdnHCl (Fig. S2 B and C).

The above measurements indicate that the values of κ^2 can range between 0.33 and 1.87 in the N state, and between 0.40 and 1.52 in the U state, leading to a maximum uncertainty of $\pm 15\%$ in the measured distances in the native state (3, 8). This value is, however, the worst case estimate and the range is expected to be narrower in view of the fact that tryptophan has multiple absorption transition dipoles, and therefore mixed polarizations (3, 5, 9). The range is expected to be even narrower when TNB is attached to the thiol, because TNB is significantly smaller in size than 1, 5-IAEDANS and is expected to have considerably less restricted motion. Hence, proceeding with the value of $\kappa^2 =$ two-thirds appears reasonable.

Mutations and Subsequent TNB Labeling Do Not Alter the Secondary Structure, Thermodynamics and Kinetics of Unfolding of MNEI.
Fig. S4 A and B show the far-UV CD spectra of the N and U states of both the mutant forms, in the unlabeled and in the TNB-labeled proteins. The overlapping far-UV CD spectra for the unlabeled and TNB-labeled forms, for both the mutant proteins, indicate that the secondary structure of MNEI is not perturbed on TNB-labeling of the sole thiol in either protein. This finding is expected as both the residue positions chosen for this study, 97 and 29, are on the surface of the protein (Fig. 1A and Fig. S1 C and D). Fig. S4 C and D show that the stabilities of the unlabeled and TNB-labeled proteins are also similar for both the mutant proteins as monitored by far-UV CD (see legend to Fig. S4). Fig. S4 C and D Insets show that the apparent rate constants of unfolding are similar for the TNB-labeled proteins and the corresponding unlabeled proteins as monitored by far-UV CD. The secondary structure, stability, and kinetics of unfolding of both the unlabeled and the corresponding TNB-labeled proteins are also similar to that of wild-type (WT) MNEI as measured previously (1). The above results suggest that the secondary structure, thermodynamics, and kinetics of unfolding of MNEI remain unperturbed on mutation and on subsequent TNB-labeling, and that the data on different mutant proteins, unlabeled as well as TNB-labeled, can be compared directly with one another.

Kinetics of Unfolding Measured by FRET.
To determine the change in FRET efficiency during unfolding, the changes in the fluorescence of the donor alone (F_D) and donor–acceptor (F_{DA})

proteins have to be monitored (Eq. S1). Several factors can, however, complicate the measurement of changes in FRET efficiencies during unfolding (4, 8, 10). These are: (i) changes in the quantum yield of the donor fluorescence; (ii) changes in acceptor-alone and donor-alone fluorescence during unfolding. These complications appear, however, to be absent in the FRET system used in this study because of the following reasons: (i) the quantum yield of the donor fluorescence does not change significantly ($\leq 5\%$) in the N and U states of unlabeled MNEI (see above); (ii) the acceptor used in this study, TNB, is not fluorescent, and hence, its fluorescence does not change during unfolding; (iii) it is observed that the donor fluorescence intensity changes only marginally at 360 nm (Fig. 1 B and C), and hence, this wavelength was chosen for the FRET experiments reported in this study. MNEI is, therefore, a good model system for studying folding/unfolding reactions using FRET, when the Trp-TNB FRET pair is used.

Fig. S6 shows the kinetics of unfolding of the unlabeled and TNB-labeled proteins, as monitored by the change in fluorescence at 360 nm. The experiments with the unlabeled and labeled proteins were carried out in an identical manner. Fig. S6 A and B show the changes in donor-alone (for Cys97) and donor–acceptor (for Cys97-TNB) fluorescence as the protein unfolds in 4 M and 6 M GdnHCl, respectively. Fig. S6 C and D do likewise for Cys29 and Cys29-TNB. For Cys97-TNB, at both the concentrations of GdnHCl, a fraction of the total change in fluorescence intensity occurs in an apparent burst phase (during the ≈ 6.2 ms dead-time of the stopped-flow instrument), followed by a single exponential increase in the fluorescence signal (Fig. S6 A and B). The fluorescence intensity increases during the unfolding reaction, because the D–A distance is expected to increase as the protein unfolds. For Cys29-TNB, it is, however, observed that the apparent burst-phase increase in the fluorescence signal is followed by a single exponential decrease in fluorescence intensity at both the concentrations of GdnHCl (Fig. S6 C and D). This observation suggests that the W4-C29TNB distance first increases and then decreases during the time-course of the unfolding reaction. The rate constant of the single exponential decrease in the fluorescence of Cys29-TNB is similar to that of the single exponential increase in fluorescence of Cys97-TNB at both the concentrations of GdnHCl. These rate constants are also similar to the rate constants of unfolding measured by far-UV CD (Fig. S5 C and D). Fig. S6 A–D also show that the donor-only fluorescence (in the unlabeled proteins) changes only marginally during the unfolding reaction. The rate constants of unfolding obtained by fitting the unfolding traces of the unlabeled proteins to a single exponential equation, however, are similar to those of the corresponding TNB-labeled proteins. In addition, the rate constants of unfolding of the unlabeled proteins were also measured from the changes in fluorescence at 340 nm (Fig. 2 E–H) and were found to be similar to the rate constant of unfolding of the corresponding TNB-labeled proteins (Fig. S5 C and D).

Given the measured changes in the fluorescence intensities in the unlabeled proteins (F_D) and in the TNB-labeled proteins (F_{DA}) (Fig. S6 A–D), and the fact that the unfolding kinetics as observed by the changes in intrinsic tryptophan fluorescence and far-UV CD were identical for each pair of unlabeled and TNB-labeled proteins, Eq. S1 could be used to generate an experimental measure of the energy transfer efficiency as a function of time, for each site. Fig. 3 A and B show the changes in FRET efficiency with the time of unfolding, both for Cys97-TNB (Fig. 3A) and Cys29-TNB (Fig. 3B).

In principle, the changes in the FRET efficiency during the unfolding of the TNB-labeled proteins can readily be transformed into changes in the D–A distances during unfolding by using Eq. S2. However, this calculation requires the knowledge of how R_0 changes with the time of unfolding. Table S1 shows

that the calculated values of R_0 in the N and U states of both TNB-labeled proteins are very similar ($R_0 = 22.8 \pm 0.2$ Å). Hence, it is justified to assume that the value of R_0 does not change during the time course of the unfolding reaction. Fig. 3 C and D show the changes in the D–A distances with the time of unfolding, both for Cys97-TNB (Fig. 3C) and Cys29-TNB (Fig. 3D).

A change in FRET efficiency is interpreted, usually, as a change in the D–A distance in all of the protein molecules. It is, however, possible that during the unfolding reaction of Cys29-TNB, the D–A distance increases first in all of the protein molecules and then contracts only in a fraction of the molecules. Steady-state FRET measurements give the ensemble-averaged change in distances and cannot distinguish between the above 2 possibilities. Time-resolved FRET experiments underway in the laboratory are expected to reveal whether all or only some molecules undergo expansion and contraction during unfolding. The important result is, however, that the D–A distance increases and then decreases in at least a substantial fraction of the unfolding molecules.

Kinetics Versus Equilibrium Amplitudes of Unfolding as Measured by FRET. Fig. S7A compares the kinetic and equilibrium amplitudes of unfolding, as measured by the change in fluorescence at 360 nm, for Cys97 as well as for Cys97-TNB. Fig. S7B does likewise for Cys29 and Cys29-TNB. For either unlabeled protein, the equilibrium values of fluorescence at 360 nm do not show a cooperative or sigmoidal dependence on the concentration of GdnHCl; instead, a linearly increasing dependence on the concentration of GdnHCl is seen, which is similar for both proteins. For either protein, the fluorescence at 360 nm increases by ≈15–20% over the entire range of GdnHCl concentration.

This dependence of the fluorescence intensity on the concentration of GdnHCl appears very similar to that of NATA (N-acetyl-L-tryptophanamide) on the concentration of GdnHCl.

For Cys97-TNB, the equilibrium values of fluorescence at 360 nm show a sigmoidal dependence on the concentration of GdnHCl (Fig. S7A). The equilibrium FRET signal increases with the increase in concentration of GdnHCl, as expected. Surprisingly for Cys29-TNB, the equilibrium FRET signal at 360 nm first increases, then decreases, and then increases again (Fig. S7B), suggesting that the W4-C29TNB distance expands and contracts during the denaturation process. The mid-point of the unfolding transition monitored by FRET is similar to that monitored by far-UV CD, for both Cys97-TNB and Cys29-TNB (Fig. S4 C and D). For both the TNB-labeled proteins, the equilibrium unfolding transitions, as monitored by FRET, display steep slopes in the native and unfolded protein baselines (Fig. S7 A and B), which suggests that both the N and U states expand gradually during unfolding.

For either TNB-labeled protein, the kinetic traces of unfolding in different concentrations of GdnHCl extrapolate, at $t = 0$, to values that fall on the linearly extrapolated native protein baseline of the equilibrium unfolding transition curve (Fig. S7 A and B). Hence, the apparent burst-phase changes seen in Fig. S6 can be attributed to the steep slopes of the native protein baselines. The slope of the linear dependence of fluorescence signal of the native protein and the kinetic $t = 0$ signals on the concentration of GdnHCl is different for the 2 TNB-labeled proteins (Fig. S7 A and B). Surprisingly, for Cys29-TNB, the kinetic $t = 0$ fluorescence signals are more than the fluorescence signals of the N and U states (Fig. S7B), suggesting that the W4-C29TNB distance in the product of the initial submillisecond burst-phase reaction is more expanded than it is in both the N and U states.

1. Patra AK, Udgaonkar JB (2007) Characterization of the folding and unfolding reactions of single-chain monellin: Evidence for multiple intermediates and competing pathways. *Biochemistry* 46:11727–11743.
2. Sinha KK, Udgaonkar JB (2005) Dependence of the size of the initially collapsed form during the refolding of barstar on denaturant concentration: Evidence for a continuous transition. *J Mol Biol* 353:704–718.
3. Lakowicz JR (2006) Energy transfer. *Principles of Fluorescence Spectroscopy*, (Springer, New York), 3rd Ed, pp 443–472.
4. Sridevi K, Udgaonkar JB (2003) Surface expansion is independent of and occurs faster than core solvation during the unfolding of barstar. *Biochemistry* 42:1551–1563.
5. Haas EE, Katchalsky-Katzir E, Steinberg IZ (1978) Effect of the orientation of donor and acceptor on the probability of energy transfer involving electronic transitions of mixed polarization. *Biochemistry* 17:5064–5070.
6. Chen R (1972) Measurements of absolute values in biochemical fluorescence spectroscopy. *J Research National Bureau Standards* 76A:593–606.
7. Mukhopadhyay S, Nayak PK, Udgaonkar JB, Krishnamoorthy G (2006) Characterization of the formation of amyloid protofibrils from barstar by mapping residue-specific fluorescence dynamics. *J Mol Biol* 358:935–942.
8. Lillo MP, Beechem JM, Szpikowska BK, Sherman MA, Mas MT (1997) Design and characterization of a multisite fluorescence energy-transfer system for protein folding studies: A steady-state and time-resolved study of yeast phosphoglycerate kinase. *Biochemistry* 36:11261–11272.
9. Garcia-Mira MM, Sadqi M, Fischer N, Sanchez-Ruiz JM, Munoz V (2002) Experimental identification of downhill protein folding. *Science* 298:2191–2195.
10. Lillo MP, Szpikowska BK, Mas MT, Sutin JD, Beechem JM (1997) Real-time measurement of multiple intramolecular distances during protein folding reactions: A multisite stopped-flow fluorescence energy-transfer study of yeast phosphoglycerate kinase. *Biochemistry* 36:11273–11281.
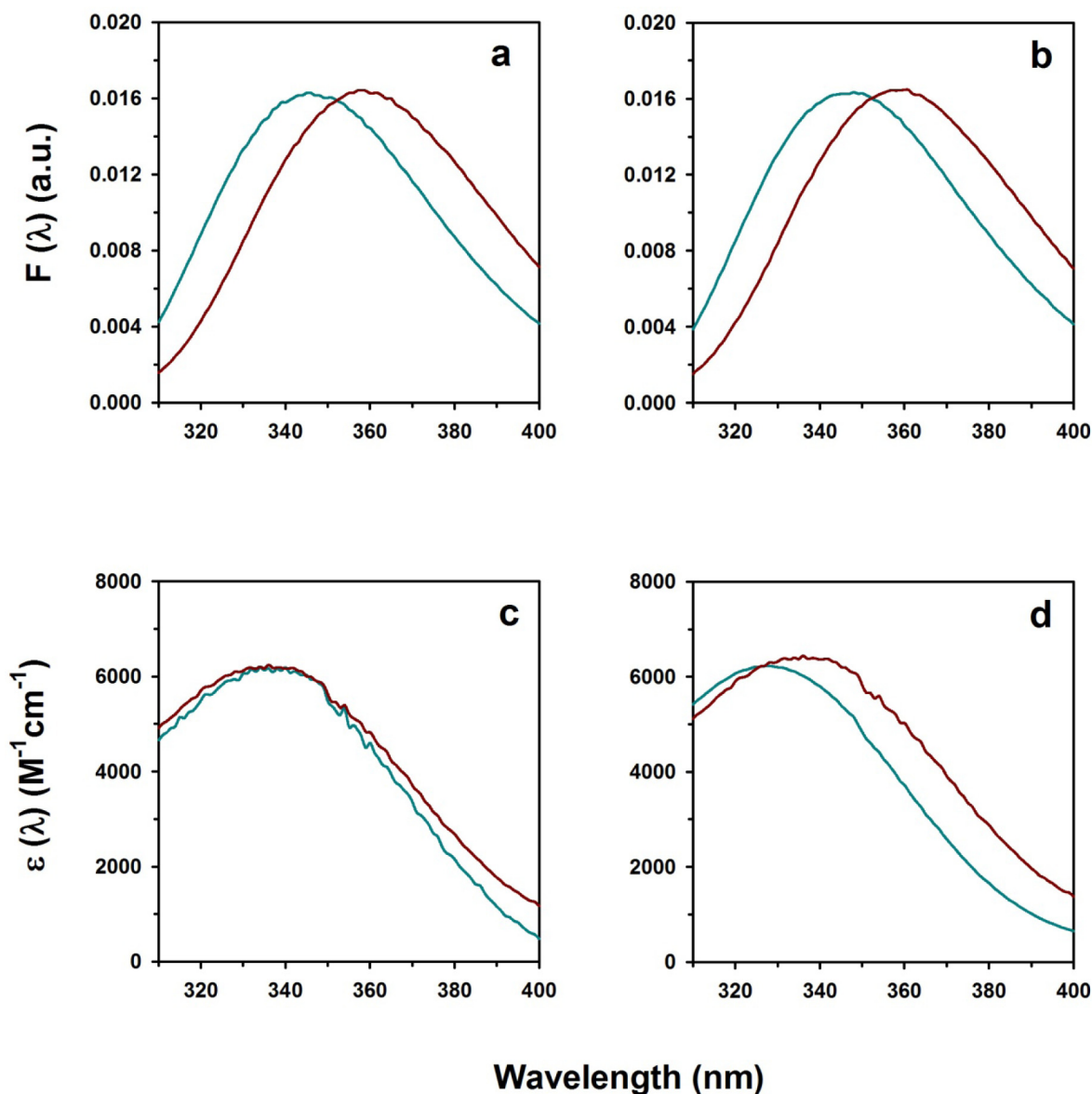
Fig. S1. Determination of the overlap integral, *J*. Fluorescence emission spectra of the donor, W4, in Cys97 (*A*) and Cys29 (*B*) are shown. In both *A* and *B*, the blue and dark red lines represent the fluorescence emission spectra, $F(\lambda)$, of the unlabeled native and unfolded proteins, respectively. Each spectrum was normalized so that the total area under the spectrum is unity. Absorbance spectra of the acceptor, TNB, in Cys97-TNB (*C*) and Cys29-TNB (*D*) are shown. In *C* and *D*, the blue and dark red lines represent the absorbance spectra, $\varepsilon(\lambda)$, of the TNB-labeled, native, and unfolded proteins, respectively. Absorbance spectra for the TNB-labeled proteins in the N and U states were collected on a CARY100 double-beam spectrophotometer with a bandwidth of 1 nm and a scan speed of 1 nm/s, using a cuvette with a path length of 1 cm. Each absorption spectrum was divided by the respective molar protein concentration to obtain $\varepsilon(\lambda)$. *J* was determined as the overlap between $F(\lambda)$ and $\varepsilon(\lambda)$ according to Eq. **S4**, where the wavelength λ is in nm.
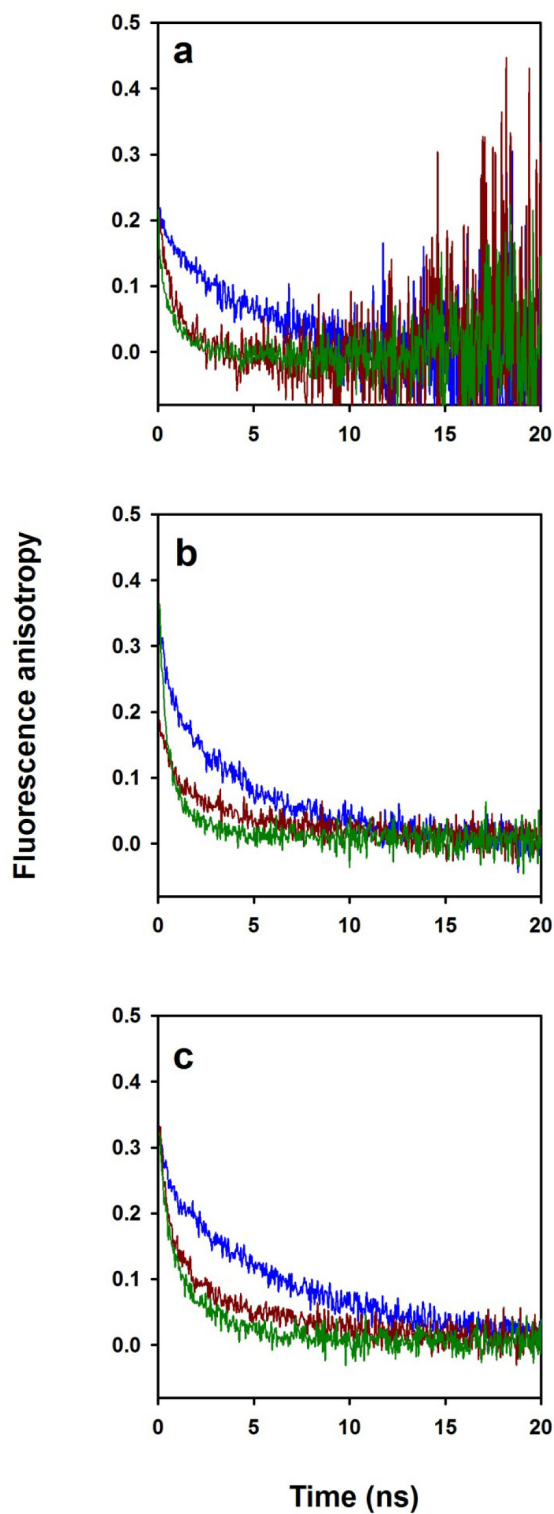
Fig. S2. The donor and the acceptors appear to rotate freely. Time-resolved fluorescence anisotropy decays of (*A*) W4; (*B*) C97-IAEDANS, and (*C*) C29-IAEDANS. In *A*–*C*, the blue, dark red, and dark green lines represent the fluorescence anisotropy decays in 0 M, 2 M, and 4 M GdnHCl, respectively. The time-resolved fluorescence anisotropy decay measurements were made by using a high-repetition-rate picosecond laser (frequency doubled Ti-sapphire laser, Tsunami; Spectra-Physics Inc.), coupled to a time-correlated single-photon counting (TCSPC) set-up, as described in ref. 7. The width (FWHM) of the instrument response function was ≈40 ps.

Fig. S3. The initial intermediate does not bind to the hydrophobic dye ANS (*A* and *C*, Cys97; *B* and *D*, Cys29). In *A–D*, the green trace corresponds to the signal of native protein mixed with unfolding buffer containing ANS; the pink trace corresponds to the signal of native protein mixed with native buffer containing ANS; and the blue trace corresponds to the signal of unfolded protein mixed with unfolding buffer containing ANS. In *A* and *B*, the final concentration of the protein after mixing is 5 μM, and that of ANS was 50 μM. In *C* and *D*, the final concentration of the protein after mixing is 50 μM, and that of ANS was 500 μM. Where unfolding buffer was used, the final concentration of GdnHCl after mixing was 4 M. *Insets* in *A–D* show the first 1 s of the data.
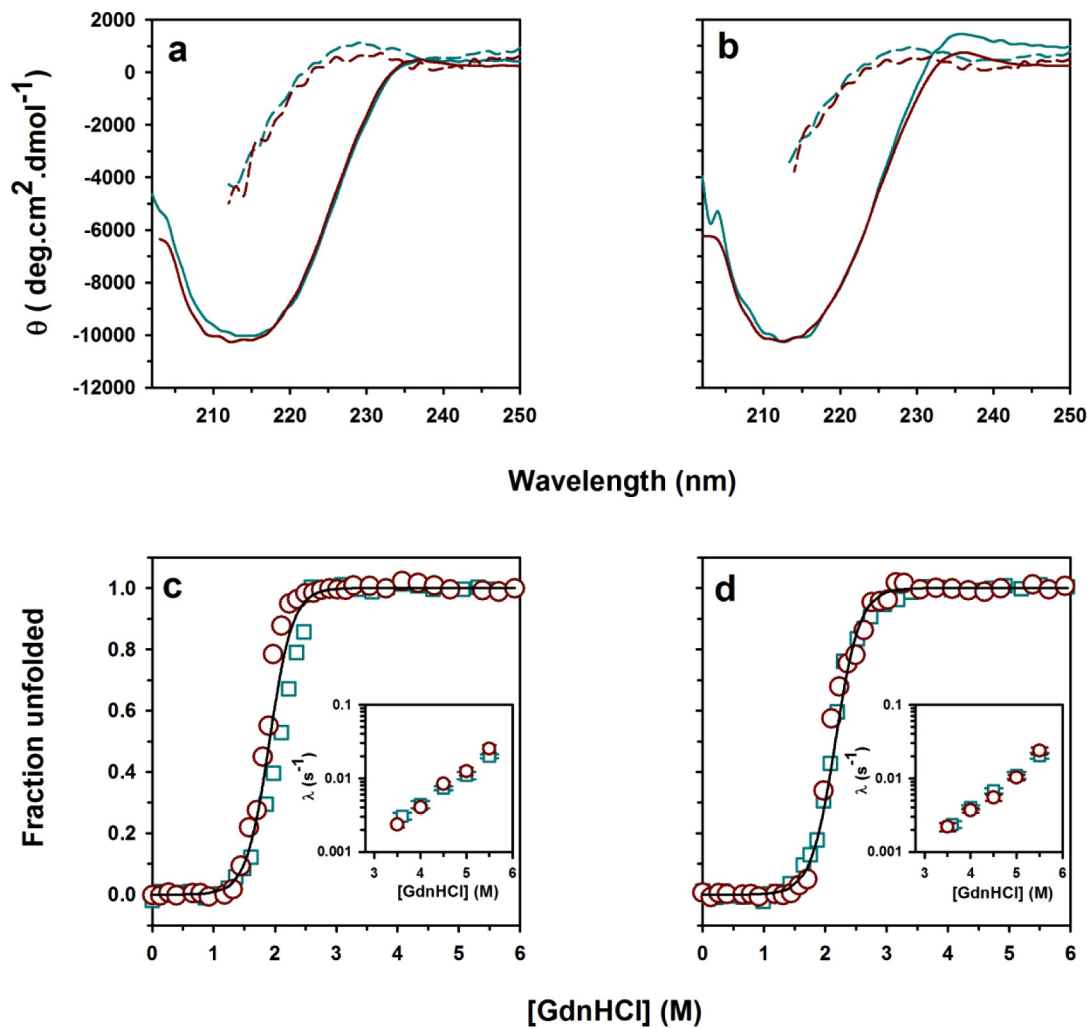
Fig. S4. The secondary structure, thermodynamics, and kinetics of unfolding of MNEI remain unperturbed on mutation and on subsequent TNB-labeling (*A* and *C*, Cys97 and Cys97-TNB; *B* and *D*, Cys29 and Cys29-TNB). *A* and *B* show the far-UV CD spectra of the unlabeled native (solid blue line), TNB-labeled native (solid dark red line), unlabeled unfolded (dashed blue line), and TNB-labeled unfolded (dashed dark red line) proteins. *C* and *D* show the equilibrium unfolding transitions of the unlabeled (blue squares) and TNB-labeled (dark red circles) proteins as monitored by the change in the CD signal at 222 nm. The fraction of unfolded protein is plotted against GdnHCl concentration. The black continuous lines through the data represent nonlinear least-squares fits to a 2-state N⇌U model. The free energy of unfolding, ΔG_U, and the mid-point of unfolding, C_m, as determined from 2-state analysis is 6.6 kcal mol^{-1} and 2.08 M for Cys97; 6.0 kcal mol^{-1} and 1.91 M for Cys97-TNB; 6.6 kcal mol^{-1} and 2.09 M for Cys29; and 6.5 kcal mol^{-1} and 2.05 M for Cys29-TNB, respectively. *Insets* in *C* and *D* show the dependence of the observed rate constants of unfolding on the concentration of GdnHCl as monitored by the change in the CD signal at 222 nm for the unlabeled (blue squares) and TNB-labeled (dark red circles) proteins.
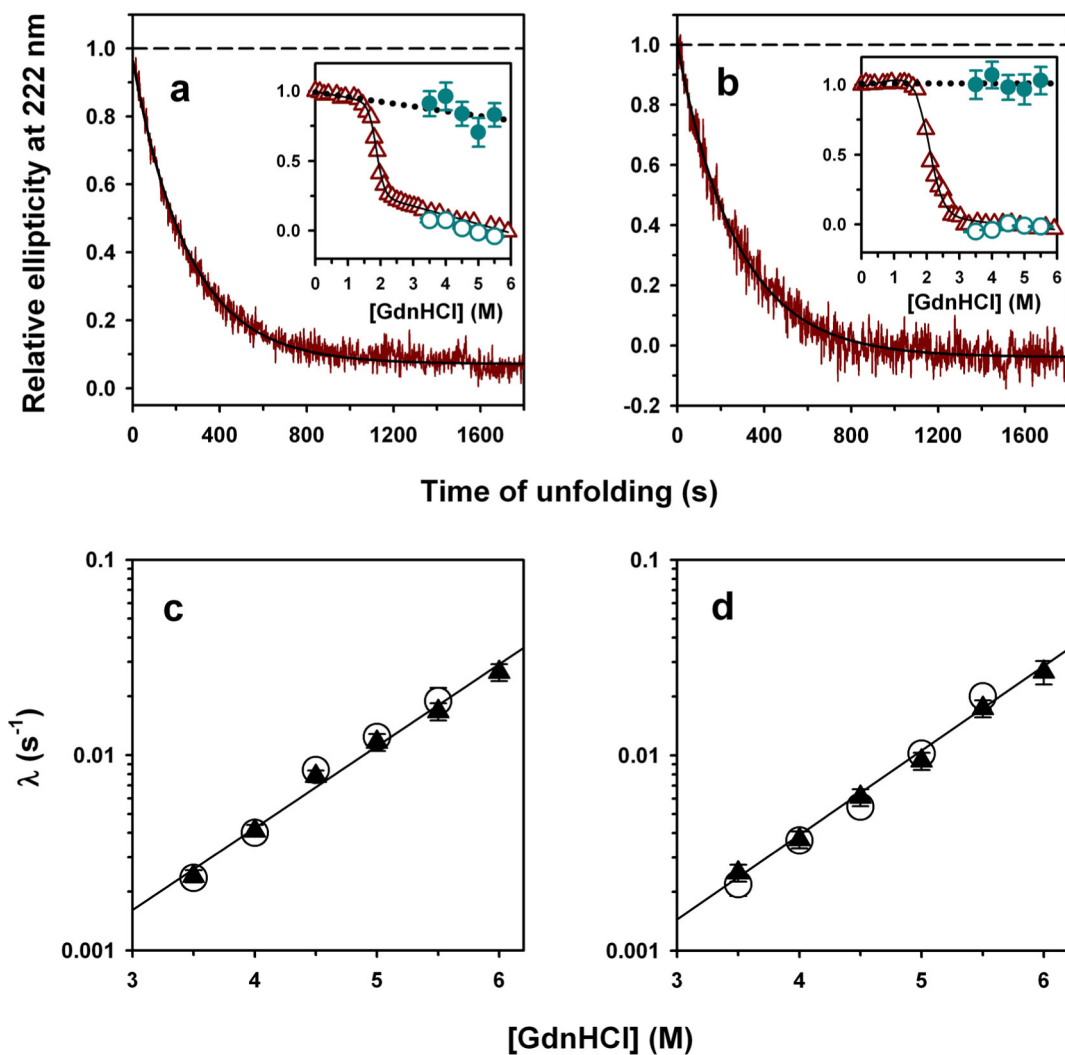
Fig. S5. Far-UV CD monitored unfolding of the TNB-labeled proteins at pH 8 and 25 °C (*A*, Cys97-TNB; *B*, Cys29-TNB). In *A* and *B*, the solid dark red lines show the kinetic traces of unfolding in 4 M GdnHCl as monitored by the change in the CD signal at 222 nm, and the black solid lines through the data are fits to a single exponential equation. The black dashed lines represent the signal of native protein. *Insets* in *A* and *B* show the kinetic versus equilibrium amplitudes of unfolding of the corresponding TNB-labeled proteins as monitored by the change in the CD signal at 222 nm. The dark red triangles represent the equilibrium unfolding transition, and the continuous line through the data represents a fit to a 2-state N⇌U model. The blue empty circles represent the $t = \infty$ signal, and the blue filled circles represent the $t = 0$ signal, respectively, obtained from fitting the kinetic traces of unfolding to a single exponential equation. The black dotted line is a linear extrapolation of the native protein baseline. *C* (Cys97-TNB) and *D* (Cys29-TNB) compare the observed rate constants of unfolding as monitored by change in far-UV CD signal at 222 nm (empty circles) and fluorescence of W4 at 360 nm (filled triangles). In *C* and *D*, the black line through the data is a straight line fit to the average of the rate constants from the 2 probes. The error bars, wherever shown, represent the standard deviations of measurements from at least 3 separate experiments.
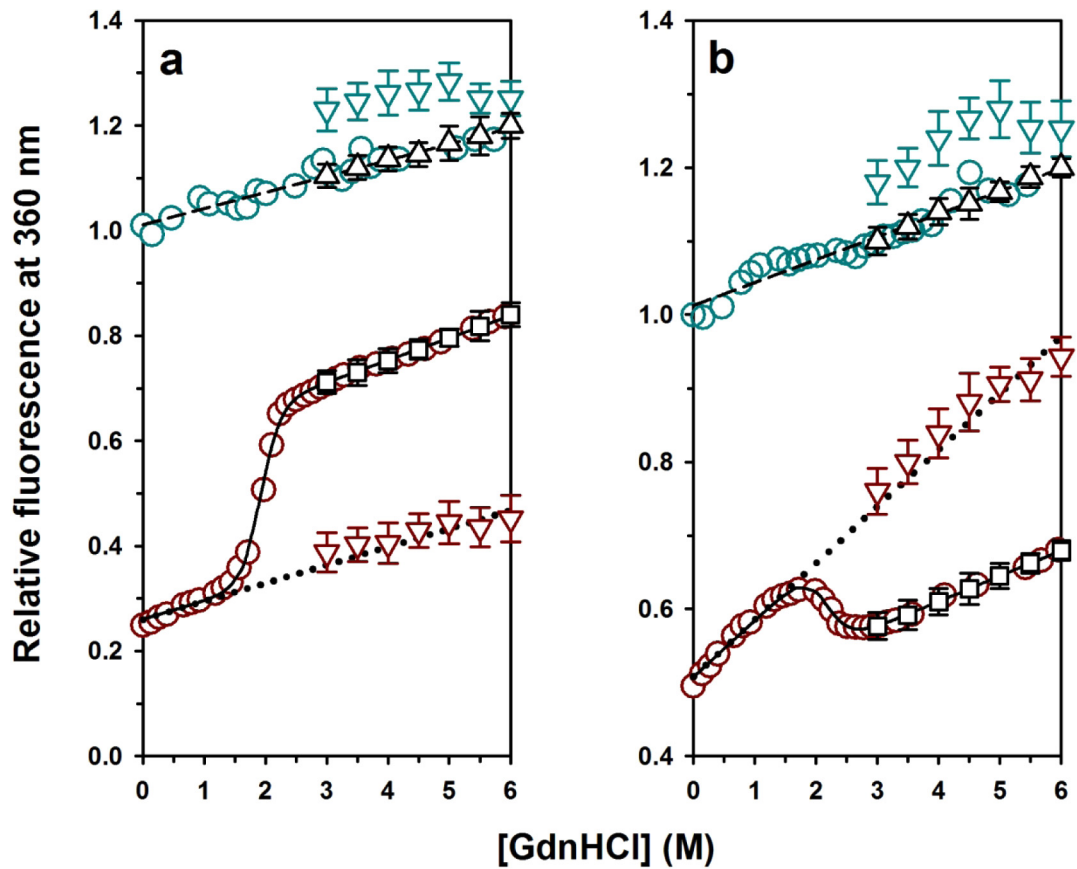
Fig. S6. Kinetics of unfolding of unlabeled and TNB-labeled proteins as monitored by the change in fluorescence intensity of W4 during unfolding at 360 nm (*A* and *B*, Cys97 and Cys97-TNB; *C* and *D*, Cys29 and Cys29-TNB; *A* and *C*, 4 M GdnHCl; *B* and *D*, 6 M GdnHCl). In *A–D*, the solid blue line and the solid dark red line represent the change in the fluorescence intensity of W4 during unfolding at 360 nm in the unlabeled and the TNB-labeled proteins, respectively. The dashed blue line and the dashed dark red line represent the fluorescence signal of W4 at 360 nm in the unlabeled and the TNB-labeled native proteins, respectively. The black solid lines are single exponential fits to the observed data. All of the data were normalized to a value of 1 for the signal of the unlabeled native protein at 360 nm.

Fig. S7. Kinetic versus equilibrium amplitudes of the unfolding of unlabeled and TNB-labeled proteins as monitored by the change in fluorescence at 360 nm (*A*, Cys97 and Cys97-TNB; *B*, Cys29 and Cys29-TNB). In *A* and *B*, the blue circles represent the equilibrium unfolding transition of the unlabeled protein, the dashed black line through the data represents a fit to a straight line equation. The blue inverted triangles and the black triangles represent the $t = 0$ and $t = \infty$ signals, respectively, obtained from fitting the kinetic traces of unfolding of the unlabeled protein to a single exponential equation. The dark red circles represent the equilibrium unfolding transition of the TNB-labeled protein, the continuous black line represents a fit to a 2-state N⇌U model, and the dotted black line is a linear extrapolation of the native protein baseline. The black squares represent the $t = \infty$ signal, and the dark red inverted triangles represent the $t = 0$ signal, obtained from fitting the kinetic traces of unfolding of the TNB-labeled protein to a single exponential equation. The error bars, where shown, represent standard deviations of the measurements from at least 3 separate experiments.

Table S1. Energy transfer parameters

FRET pair	FRET efficiency*		Overlap integral[†] $J \times 10^{-13}$, $M^{-1}cm^{-1}nm^4$		Förster's distance,[‡] R_0, Å		D–A distance in N, Å	
	N	U	N	U	N	U	by FRET[§]	Calculated[¶]
W4-C97TNB	0.75	0.15	6.1	6.9	22.9	22.6	19.1	17.6
W4-C29TNB	0.51	0.40	6.0	7.2	23.0	22.8	22.8	24.2

*The fluorescence resonance energy transfer efficiency is determined using the fluorescence spectra in Fig. 1 *B* and *C* and by using Eq. **S1**. The value of the fluorescence at 360 nm for the unlabeled protein was taken as F_D, and the value of the fluorescence at 360 nm for the corresponding TNB-labeled protein was taken as F_{DA}.

[†]*J* was calculated using Eq. **S4**.

[‡]R_0 was determined using Eq. **S3** and the following values: κ^2 = two-thirds; *n* = 1.33 for N and 1.4 for U; and Q_D = 0.133 for N and 0.128 for U.

[§]D–A distances were calculated using Eq. **S2**.

[¶]Average distance between the side-chains of the 2 residues calculated from the X-ray structure of MNEI. The size of the TNB adduct is not included.